npg

ARTICLE

Efficient gene delivery to photoreceptors using AAV2/rh10 and rescue of the Rho−/− mouse

Arpad Palfi[1], Naomi Chadderton[1], Mary O'Reilly[1], Kerstin Nagel-Wolfrum[2], Uwe Wolfrum[2], Jean Bennett[3], Peter Humphries[1], Paul Kenna[1], Sophia Millington-Ward[1] and Jane Farrar[1]

As gene therapies for various forms of retinal degeneration progress toward human clinical trial, it will be essential to have a repertoire of safe and efficient vectors for gene delivery to the target cells. Recombinant adeno-associated virus (AAV) serotype 2/2 has been shown to be well tolerated in the human retina and has provided efficacy in human patients for some inherited retinal degenerations. In this study, the AAV2/8 and AAV2/rh10 serotypes have been compared as a means of gene delivery to mammalian photoreceptor cells using a photoreceptor specific promoter for transgene expression. Both AAV2/8 and AAV2/rh10 provided rescue of the retinal degeneration present in the rhodopsin knockout mouse, with similar levels of benefit as evaluated by molecular, histological, and functional readouts. Transgene expression levels were significantly higher (fivefold) 1 week postsubretinal injection when employing AAV2/8 for rhodopsin gene delivery compared to AAV2/rh10, and were indistinguishable by 6 weeks postadministration of vector. This study reports the use of the AAV2/rh10 serotype to provide rescue in a degenerating retina and provides a comparative evaluation of AAV2/rh10 with respect to AAV2/8, a serotype regarded as providing efficient delivery to photoreceptors.

INTRODUCTION

Gene therapies for ocular disorders have been spearheaded by clinical trials for Leber congenital amaurosis (LCA) linked to *RPE65*. Notably, gene replacement of the *RPE65* gene provided benefit in patients with this early-onset retinal dystrophy.[1–3] The success of the LCA trials is not only relevant in its own context but has also greatly advanced the wider ocular gene therapy field. Significantly, these trials showed not only some efficacy, but also importantly the tolerance of the eye to the delivery vector, an adeno-associated virus (AAV). This small nonpathogenic parvovirus can transduce many cell types including nondividing terminally differentiated cells such as neurons. The eye has proved to be an excellent model organ for gene therapy treatment because of its accessible nature and its immune privileged state.[4,5] The value of AAV for gene delivery to the retina has been further supported by a recent phase 1 trial for Choroideremia in which beneficial effects were obtained.[6]

A number of hybrid AAV vectors have been engineered with different AAV capsid proteins to provide different tropisms and optimal transduction efficiencies for various target cell types.[7–17] In the retina, AAV tropism has been assessed and transduction efficiencies in different cell types compared.[7,8,10,13,18–21] It has been found that a number of AAV serotypes transduce retinal pigment epithelial (RPE) cells (AAV 2/1, 2/2, 2/5, 2/7, 2/8, and 2/9) and horizontal cells (2/1, 2/2, 2/8, 2/9, and 2/10) efficiently. Photoreceptor cells are readily transduced by serotypes 2/1, 2/5, 2/7, 2/8, 2/9, and 2/11

following subretinal injection, with AAV 2/8 regarded as the most efficient in this cell type.[1,13,20,22] For some retinal cell types, such as bipolar, ganglion or glial cells, where existing AAV serotypes may not be particularly efficient, methodologies such as directed evolution have been employed to generate novel serotypes which may provide vectors with predilections for these cells.[14–16]

AAV2/rh10, used in this study, was isolated from nonhuman primates (NHPs) by polymerase chain reaction (PCR) amplification of latent genomes.[9] Neither the receptor for AAV2/rh10 has been identified, nor the tropism of this capsid serotype fully elucidated but it has been shown to efficiently transduce cells of the central nervous system. Cearley and Wolfe[23] demonstrated that AAV2/rh10 can transduce neurons, with greater efficacy than AAV2/7, 2/8, and 2/9 in adult mouse brains. Hu *et al.*[24] reported that reporter gene expression was ~20-fold higher when transduced with AAV2/rh10 compared with AAV2/8 in murine brain transduced at p2. Long-term expression and safety of AAV2/rh10 has also been observed in the brains of rats and NHPs.[25] In addition, AAV2/rh10 has been shown to transduce some retinal cell types including ganglion cells and RPE cells following intravitreal injection.[26] An AAV2/rh10 expressing an antihuman vascular endothelial growth factor antibody transgene, Bevacizumab, has also been shown to transduce RPE cells, when administered intravitreally, and to suppress neovascularization in a murine model for age-related macular degeneration.[27] In addition, Watanabe *et al.*[20] demonstrated efficient AAV2/rh10-mediated

The first two authors and the last two authors contributed equally to this work.

[1]Department of Genetics, School of Genetics and Microbiology, Trinity College Dublin, Dublin 2, Ireland; [2]Cell and Matrix Biology, Institute of Zoology, Johannes Gutenberg-Universität Mainz, Mainz, Germany; [3]Center for Advanced Retinal and Ocular Therapeutics, Perelman School Of Medicine, University of Pennsylvania, Philadelphia, Pennsylvania, USA. Correspondence: A Palfi (palfia@tcd.ie)

npg

Gene delivery to photoreceptors using AAV2/rh10
A Palfi *et al*.

2

transduction of horizontal and ganglion cells following postnatal day (p) 0 subretinal injection; however, inefficient transduction of photoreceptors was obtained in this study.

Because retinal degenerations frequently originate from genetic mutations primarily affecting photoreceptors, it is pertinent to identify vectors that efficiently transduce and express gene therapies in these cells. Given the potency of AAV2/rh10 to transduce neurons, including some retinal cell types, it was of value to address whether this serotype might target photoreceptors efficiently and, moreover, might provide clinically relevant benefit in a murine model of retinal degeneration. Earlier, we established significant rescue of the severe retinal degeneration present in a rhodopsin knockout mouse ($Rho^{-/-}$[28]) when delivering a human rhodopsin (*RHO*) transgene via AAV2/5.[29] Improvement in the retention of rod photoreceptor cells and retinal architecture as well as retinal function was achieved in this study. In order to evaluate the efficacy of photoreceptor rescue using the AAV2/rh10 serotype in this study, we re-employed the $Rho^{-/-}$ murine model and expressed an efficient *RHO* replacement construct,[29] which utilizes an optimized murine rhodopsin promoter (BB24; Figure 1a). As AAV2/8 is considered to be one of the most efficient serotypes for targeting photoreceptors in rodents, the efficacy of AAV2/rh10 transduction was directly compared to that of AAV2/8. Significant benefit was obtained from *RHO* replacement utilizing both AAV2/rh10 and AAV2/8 delivery via subretinal administration in this study. Of note this study reports an AAV2/rh10-based gene therapy approach providing benefit to photoreceptor cells in a degenerating retina.

RESULTS

In order to compare the utility of AAV2/8 and AAV2/rh10 in photoreceptor gene therapy applications, the effects of rhodopsin gene
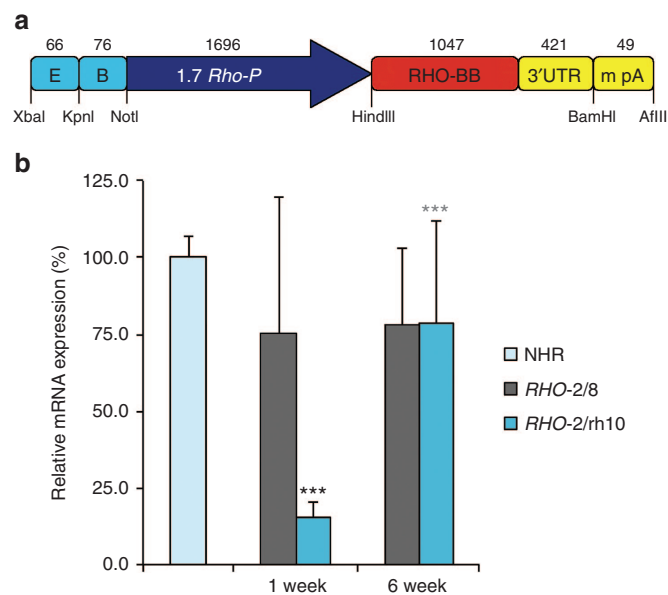
Figure 1 *RHO* replacement construct and *RHO* mRNA expression *in vivo*. An efficient rhodopsin replacement construct, *i.e.*, BB24 (**a**) as described in ref. 29, was produced as AAV2/8-BB24 (*RHO*-2/8) and AAV2/rh10-BB24 (*RHO*-2/rh10). (**b**) Eyes of *Rho*–/– mice were subretinally injected with 5×10^9 vg/eye of either *RHO*-2/8 or *RHO*-2/rh10 at p3-4 ($n = 8$–10). Retinas were harvested and *RHO* mRNA expression analyzed by RT-qPCR 1 and 6 weeks postinjection. β-Actin was used as an internal control. Relative expression levels are given as a percentage of levels in 3-month-old NHR+/– *Rho*–/– retinas ($n = 4$). ***$P < 0.001$ between *RHO*-2/8 and *RHO*-2/rh10 at 1 week; ***$P < 0.001$ between *RHO*-2/rh10 at 1 and 6 weeks.

replacement were analyzed in transgenic mice with a targeted disruption in the rhodopsin gene ($Rho^{-/-}$ mice[28]) employing AAV2/8 or AAV2/rh10 for delivery. In the absence of rhodopsin, $Rho^{-/-}$ mice neither develop rod outer segments (OS) nor have a detectable rod-derived electroretinogram (ERG) at any stage of development. Because of the progressive loss of rods, the outer nuclear layer (ONL) has only one layer (of mostly cones) remaining by 3 months of age and no ONL at all by 6 months of age. Earlier, we utilized the $Rho^{-/-}$ model to optimize a rhodopsin replacement strategy employing AAV2/5; rescue of retinal structure and function was achieved in this study.[29] An effective rhodopsin replacement construct from this study (BB24, Figure 1a) was packaged into AAV2/8 (ref. 10) and AAV2/rh10 (ref. 9) for use in this study, generating AAV2/8-BB24 (*RHO*-2/8) and AAV2/rh10-BB24 (*RHO*-2/rh10).

Eyes of p3-4 $Rho^{-/-}$ pups were subretinally injected with 5×10^9 vg/eye of either *RHO*-2/8 or *RHO*-2/rh10 in a 0.6 μl volume. To enable transduction to be monitored, both AAV vectors were mixed with 1×10^8 vg/eye of AAV-EGFP (enhanced green fluorescent protein[29]) prior to injection; untreated eyes served as controls. Using these parameters, the transduced area (based on native EGFP fluorescence) was ~40–60% of the retina (see Supplementary Figure S1). Molecular, structural, and functional analyses of the retinas were undertaken using reverse transcription-quantitative real-time PCR (RT-qPCR), light and electron microscopy, ERG, and optometry.

RHO mRNA expression

Total RNA was isolated from 3-month-old NHR+/– $Rho^{-/-}$ retinas[28,30] ($n = 4$) and transduced $Rho^{-/-}$ retinas 1 and 6 weeks postdelivery of either *RHO*-2/8 or *RHO*-2/rh10 ($n = 8$–10). *RHO* mRNA expression was determined using RT-qPCR; β-actin mRNA expression was used as an internal control. Relative *RHO* mRNA levels normalized to expression in NHR+/– $Rho^{-/-}$ retinas are provided in Figure 1b. At 1 week postinjection, *RHO* expression levels from *RHO*-2/rh10 injected retinas ($15.5 \pm 5.1\%$) were approximately fivefold lower than from *RHO*-2/8 injected eyes ($75.4 \pm 44.1\%$), $P < 0.001$. At 6 weeks, no increase in expression from *RHO*-2/8 was observed compared to *RHO*-2/8 at 1 week. In contrast, significant increases in expression were observed with *RHO*-2/rh10 between 1 and 6 weeks ($78.8 \pm 33.0\%$; $P < 0.001$; Figure 1b) such that expression levels of rhodopsin were not significantly different for the *RHO*-2/rh10 and *RHO*-2/8 serotypes by 6 weeks postinjection. Notably, expression levels of rhodopsin in $Rho^{-/-}$ retinas treated with *RHO*-2/rh10 and *RHO*-2/8 were ~75% of that in adult NHR+/– $Rho^{-/-}$ retinas 6 weeks postinjection. The difference between expression levels in NHR+/– $Rho^{-/-}$ and treated $Rho^{-/-}$ retinas was not statistically significant because of the high variation in the treated samples.

Histology

Histological analysis using light microscopy was undertaken at 3 and 6 months postinjection; the architecture of the photoreceptor layer, rhodopsin expression, and the general structure of the retina were evaluated (Figures 2–4). At 3 months postinjection, the thickness of the ONL was 27.6 ± 5.5 μm ($n = 4$), 25.8 ± 7.2 μm ($n = 4$), and 4.4 ± 0.9 μm ($n = 5$) in *RHO*-2/8 or *RHO*-2/rh10 treated and control eyes, respectively (Figure 2a,b,c,g). The ONL thickness in the AAV-treated eyes was significantly greater than that of the control eyes ($P < 0.05$), whereas the ONL thickness was not statistically different between *RHO*-2/8- and *RHO*-2/rh10-treated eyes. At 6 months postinjection, the thickness of the ONL was 21.9 ± 6.7 μm ($n = 6$) and 24.9 ± 4.1 μm ($n = 6$) in *RHO*-2/8- or *RHO*-2/
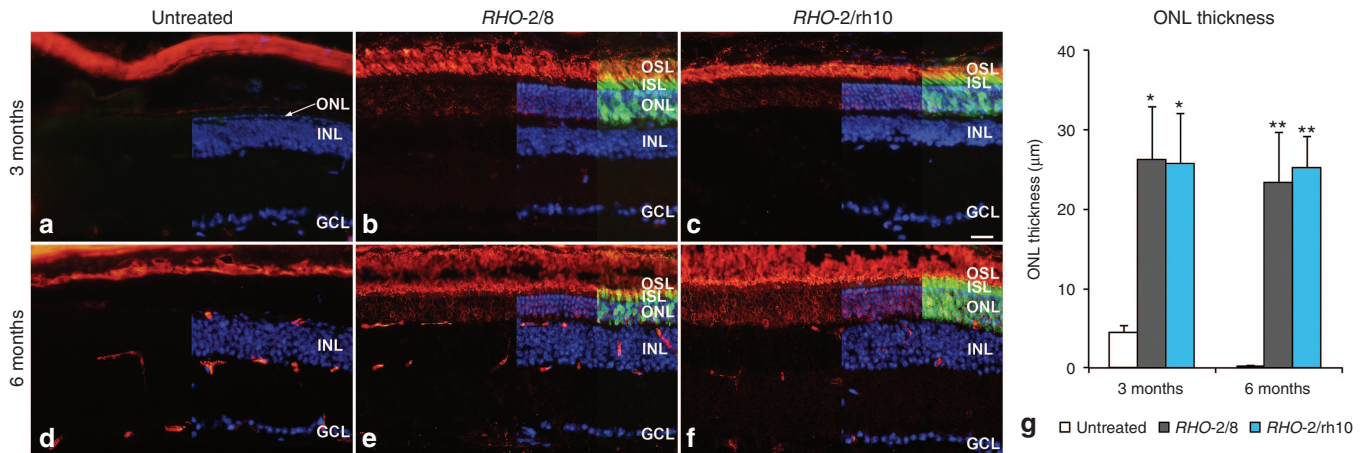
Figure 2 Immunohistochemical analysis of *RHO* expression in *RHO*-2/8 and *RHO*-2/rh10 transduced retinas in *Rho*–/– mice. Eyes of *Rho*–/– mice were subretinally injected with 5×10^9 vg/eye of either (**b** and **e**) AAV2/8-BB24 (*RHO*-2/8) or (**c** and **f**) AAV2/rh10-BB24 (*RHO*-2/rh10) at p3-4. Both AAVs were mixed with 1×10^8 vg/eye of AAV2/5-EGFP tracer; (**a** and **d**) untreated eyes served as controls. Eyes were fixed and processed for immunohistochemistry using 4D2 antirhodopsin primary and Cy3-conjugated secondary antibodies 3 (**a–c**) and 6 months (**d–f**) postinjection; nuclei were counterstained with DAPI ($n = 4$–6). (**a–f**) Representative fluorescent microscope images illustrate rhodopsin immunohistochemical labeling (red), native EGFP fluorescence (green), and DAPI signal (blue) overlaid. Note that DAPI and EGFP signals were overlaid on the right half and right quarter of the images, respectively. The thickness of the ONL was measured; mean values of ONL thickness are given in a bar chart (**g**). Error bars represent SD values. INL: inner nuclear layer; GCL: ganglion cell layer; ISL: photoreceptor IS layer; OSL: photoreceptor OS layer; scale bar (panel **c**): 25 μm; *$P < 0.05$ and **$P < 0.001$ compared with corresponding untreated controls.
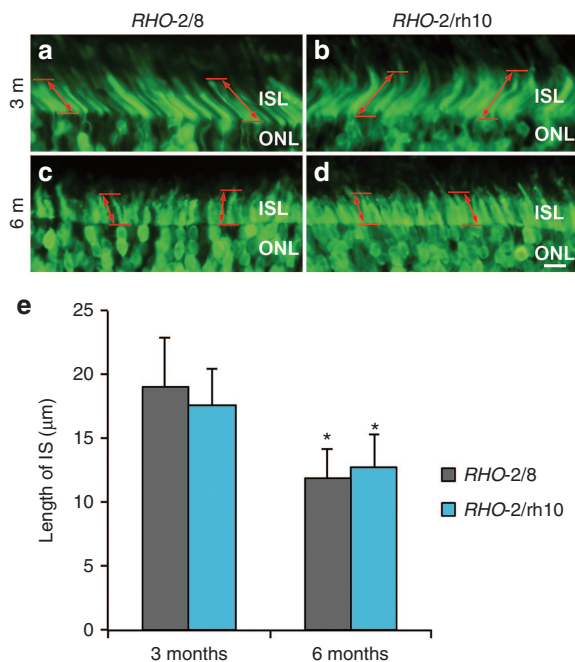

Figure 3 Photoreceptor segments in *RHO*-2/8 and *RHO*-2/rh10 transduced retinas in *Rho*–/– mice. Eyes of *Rho*–/– mice were subretinally injected with 5×10^9 vg/eye of either (**a** and **c**) AAV2/8-BB24 (*RHO*-2/8) or (**b** and **d**) AAV2/rh10-BB24 (*RHO*-2/rh10) at p3-4. Both AAVs were mixed with 1×10^8 vg/eye of AAV2/5-EGFP tracer; untreated eyes served as controls (not shown). Eyes were fixed and processed for fluorescent microscopy ($n = 3$–6) 3 (**a** and **b**) and 6 (**c** and **d**) months postinjection. Representative microscope images **a–d** illustrate native EGFP fluorescence (green) at the boundary of the ONL and the photoreceptor inner segment layer (ISL). The length of inner segments (IS) was measured and mean values of IS length are given in a bar chart (**e**). Error bars represent SD values. Scale bar (panel **d**): 10 μm; *$P < 0.05$ between 3- and 6-month postinjections.

rh10-treated eyes, respectively (Figure 2d–g). The untreated *Rho*–/– (control) eyes had no ONL remaining ($n = 5$). The thickness of ONL was not statistically different between *RHO*-2/8- or

RHO-2/rh10-treated eyes. However, all the AAV-treated eyes had a significantly thicker ONL than the untreated *Rho*–/– (control) eyes ($P < 0.01$). The ONL thickness in the *RHO*-2/8- and *RHO*-2/rh10-treated eyes did not differ significantly between 3 and 6 months postinjection. In the transduced areas of both *RHO*-2/8 and *RHO*-2/rh10 (at 3 and 6 months postinjection), rhodopsin immunolabeling was detected in the OS and to a lesser extent in the photoreceptor cell bodies (Figure 2b,c,e,f); no labeling was observed in the untreated *Rho*–/– retinas (Figure 2a,d).

As EGFP is transported to the photoreceptor inner segments (ISs), EGFP labeling enabled measurement of the length of the IS in the transduced area of the retinas (Figure 3). At 3 months postinjection, the length of the IS was 19.0 ± 4.0 μm ($n = 3$) and 17.7 ± 2.9 μm ($n = 3$) in *RHO*-2/8- or *RHO*-2/rh10-treated retinas, respectively; they were not statistically different from each other (Figure 3a,b,e). At 6 months postinjection, the length of the IS was 12.0 ± 2.2 μm ($n = 6$) and 12.7 ± 2.7 μm ($n = 5$) in *RHO*-2/8- or *RHO*-2/rh10-treated retinas (Figure 3c,d,e), respectively; they were not statistically different from each other but were shorter from corresponding values at 3 months (Figure 4e; $P < 0.05$). In comparison, the length of the IS was 23.8 ± 2.3 μm ($n = 3$) in the B6-EGFP (C57BL/6-Tg(CAG-EGFP)1Osb/J; stock number 003291; The Jackson Laboratory, Bar Harbor, ME) mouse at 6 months of age (data not shown). The B6-EGFP mice have normal retinas in which EGFP is expressed from the chicken β-actin promoter and cytomegalovirus enhancer and is present in the IS, thereby enabling comparison of the IS between B6-EGFP and AAV-treated *Rho*–/– mice.

In order to analyze if the AAV treatment was well tolerated, the general structure of the retinas was also evaluated by hematoxylin and eosin staining at 3 and 6 months postinjection ($n = 4$–5; Figure 4). Apart from the beneficial changes in the architecture of the photoreceptor segments and ONL, no other changes were observed. In particular, no increase in the number of infiltrates was detected in *RHO*-2/8- (Figure 4b,e) or *RHO*-2/rh10- (Figure 4c,f) transduced retinas when compared with untreated controls (untreated, Figure 4a,d).

Ultrastructural analysis was performed 6 months postinjection ($n = 2$; Figures 5 and 6). In the retina of untreated *Rho*–/– mice, only

membranous debris was detected between the RPE and the inner nuclear layer, and no ONL was present (Figure 5a,d). Both *RHO*-2/8 (Figure 5b,e) and *RHO*-2/rh10 (Figure 5c,f) transduction resulted not only in the preservation of rod photoreceptors nuclei (ONL), but also in the formation and survival of rod photoreceptor OS, which extended to the RPE. Note that OS is not present in the untreated *Rho*^{−/−} retina at any stage. In contrast, clear OS structures were evident and contained correctly formed membrane disks in the *RHO*-2/8- (Figure 6c,d) and *RHO*-2/rh10- (Figure 6g,h) treated *Rho*^{−/−} retinas. Connecting cilia with normal structure was also detected in these retinas (Figure 6b,f).

ERG

ERGs were recorded at 2, 5, and 11 months postinjection; pure rod-derived b-waves (Figure 7) and mixed rod/cone a-waves (see Supplementary Figure S2) are presented. At 2 months postinjection, means of pure rod-derived b-wave amplitudes of 219.9 ± 60.1 µV ($n = 8$) and 218.5 ± 62.7 µV ($n = 8$) were recorded for *RHO*-2/8 (Figure 7a) and *RHO*-2/rh10 (Figure 7b), respectively. These were not statistically different from each other. At 5 months postinjection, means of b-wave amplitudes of 190.3 ± 105.5 µV ($n = 4$) and 146.9 ± 38.1 µV ($n = 8$) were recorded for *RHO*-2/8 (Figure 7a) and *RHO*-2/rh10 (Figure 7b), respectively. These were not statistically different from each other but they were noticeably lower than the corresponding 2-month values; in the case of *RHO*-2/rh10, the corresponding values at 2 and 5 months postinjection differed significantly ($P < 0.05$; Figure 7). At 11 months postinjection, means of b-wave amplitudes of 90.5 ± 24.8 µV ($n = 8$) and 79.8 ± 16.5 µV ($n = 4$) were recorded for *RHO*-2/8 (Figure 7a) and *RHO*-2/rh10 (Figure 7b), respectively. These were not statistically different from each other but were different from their corresponding values at 2 months postinjection ($P < 0.001$ and <0.01 for *RHO*-2/8-treated and *RHO*-2/rh10-treated eyes, respectively; Figure 7). Note that the untreated *Rho*^{−/−} (control) eyes had no recordable rod-derived ERGs at any of the above-mentioned ages investigated (not shown).

At 2 months postinjection, means of mixed rod/cone a-wave amplitudes of 83.4 ± 16.5 µV ($n = 8$) and 82.4 ± 29.7 µV ($n = 8$) were recorded for *RHO*-2/8 and *RHO*-2/rh10 respectively (see Supplementary Figure S2). These were not statistically different from each other. At 5 months postinjection, means of a-wave amplitudes of 54.8 ± 29.2 µV ($n = 4$) and 43.8 ± 8.8 µV ($n = 8$) were recorded for *RHO*-2/8 and *RHO*-2/rh10 respectively (see Supplementary Figure S2). These were not statistically different from each other but were noticeably lower than corresponding 2 month values; in the case of *RHO*-2/rh10 the corresponding values at 2 and 5 months postinjection differed significantly ($P < 0.05$; see Supplementary Figure S2). At 11 months postinjection, means of a-wave amplitudes of 27.5 ± 14.3 µV ($n = 8$) and 20.1 ± 6.5 µV ($n = 4$) were recorded for *RHO*-2/8 and *RHO*-2/rh10, respectively (see Supplementary Figure S2); again these were not statistically different from each other but were different from corresponding values at 2 months postinjection ($P < 0.001$).

Optomotry

Functional vision was tested using a virtual optokinetic system[31] 6 months postinjection. Using the optokinetic tracking response, the spatial frequency threshold (the spatial frequency of the grating at 100% contrast where tracking behavior is no longer observed) was determined as 0.309 ± 0.017 cyc/deg ($n = 7$) and 0.328 ± 0.062 cyc/deg ($n = 6$) for *RHO*-2/8- and *RHO*-2/rh10-transduced eyes (Figure 8). The spatial frequency thresholds were 0.427 ± 0.009 cyc/deg ($n = 6$) for wild-type mice while untreated *Rho*^{−/−} mice exhibited no tracking behavior ($n = 6$; Figure 8). Differences between *RHO*-2/8- and *RHO*-2/rh10-transduced eyes were not statistically significant; however, tracking responses between AAV-treated eyes compared with wild-type or control *Rho*^{−/−} (untreated) eyes were significant ($P < 0.01$, Figure 8).

DISCUSSION

As the AAV constructs employed in this study utilize a rhodopsin promoter to drive transgene expression only in photoreceptor cells,
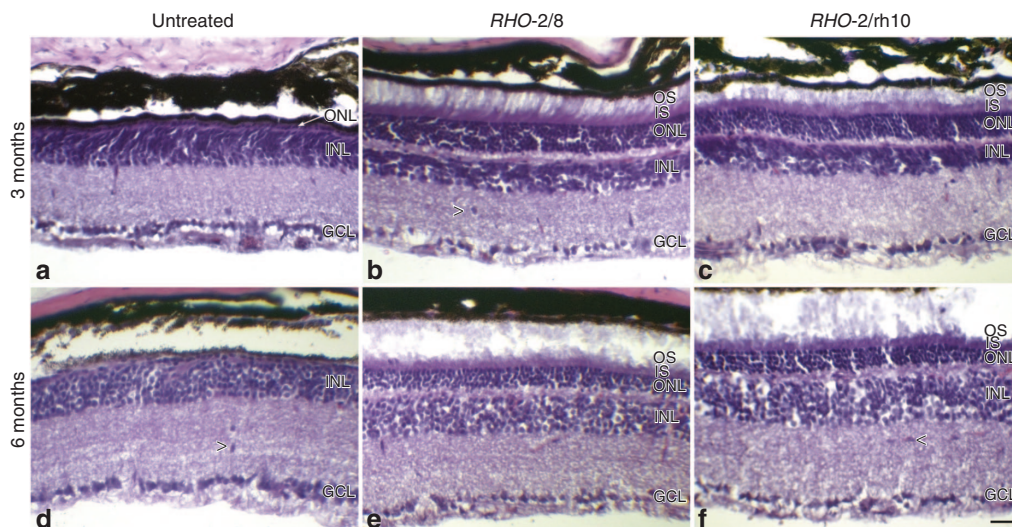

Figure 4 Analysis of retinal morphology following hematoxylin and eosin staining in *RHO*-2/8 and *RHO*-2/rh10 transduced retinas in *Rho*−/− mice. Eyes of *Rho*−/− mice were subretinally injected with 5×10^9 vg/eye of either (**b** and **e**) AAV2/8-BB24 (*RHO*-2/8) or (**c** and **f**) AAV2/rh10-BB24 (*RHO*-2/rh10) at p3-4. Both AAVs were mixed with 1×10^8 vg/eye of AAV2/5-EGFP tracer; (**a** and **d**) untreated eyes served as controls. Eyes were fixed and processed for hematoxylin and eosin staining ($n = 4$–6) 3 (**a–c**) and 6 (**d–f**) months postinjection. Representative microscope images illustrate the retinal architecture in these eyes. INL, inner nuclear layer; GCL, ganglion cell layer; ISL, photoreceptor inner segment layer; OSL, photoreceptor outer segment layer; ONL, outer nuclear layer; scale bar (panel **b**: 25 µm; arrowheads indicate cellular infiltrates (panels **b**, **d**, and **f**).
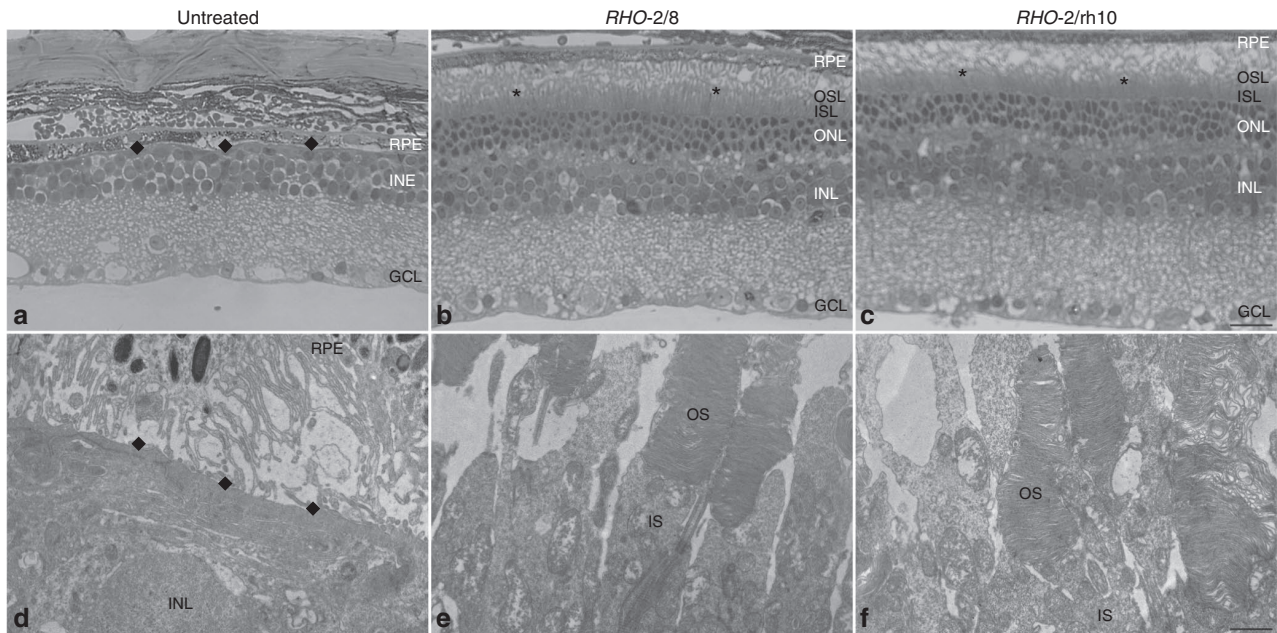
Figure 5 Ultrastructural analysis of retinas transduced with *RHO*-2/8 and *RHO*-2/rh10 in *Rho*–/– mice. Eyes of *Rho*–/– mice were subretinally injected with 5×10^9 vg/eye of either (**b** and **e**) AAV2/8-BB24 (*RHO*-2/8) or (**c** and **f**) AAV2/rh10-BB24 (*RHO*-2/rh10) at p3-4. Both AAVs were mixed with 1×10^8 vg/eye of AAV2/5-EGFP tracer; (**a** and **d**) untreated eyes served as controls. Eyes were fixed and retinas were whole mounted 6 months postinjection. Transduced areas of the retinas were identified by EGFP fluorescence, and representative areas were excised, postfixed, and further processed for transmission electron microscopy. Semi- and ultrathin sections were analyzed by light (**a–c**) and transmission electron microscopy (**d–f**), respectively. GCL, ganglion cell layer; INL, inner nuclear layer; IS, rod inner segment; ISL, inner segment layer; OS, rod outer segment; OSL, outer segment layer; RPE, retinal pigment epithelium; *photoreceptor segments; ◆, RPE/INL boundary; scale bar (panel c): 25 μm; scale bar (panel f): 1 μm.

a controlled comparative evaluation of the efficiency of transgene expression specifically in murine photoreceptors was undertaken. Using this approach we demonstrated the capacity of AAV2/rh10 to target mammalian photoreceptors efficiently following subretinal injection, attaining levels of transduction equal to AAV2/8. Indeed, the results suggest that both AAV2/8 and AAV2/rh10 provided similar levels of rescue of the retinal degeneration observed in *Rho*–/– mice. Earlier, we described the benefit in the *Rho*–/– model using an AAV2/5 serotype for gene delivery.[29] In that study, doses of AAV2/5 in a similar range to this study were employed. Notably, a similar magnitude of rescue was observed between the studies; therefore AAV2/5, AAV2/8, and AAV2/rh10 have now been shown in a murine retinal degeneration model to provide similar levels of efficacy following photoreceptor transduction. As AAV transduction is species-dependent, it remains to be established whether the efficacy of these serotypes established in mice directly translates to the humans. In this regard, it is notable that for other neuronal tissues such as motor neurons, AAV2/rh10 outperformed AAV serotypes such as AAV2 and AAV8, and moreover, the efficient transduction obtained in mice with AAV2/rh10 translated through to NHPs.[32] The results from this study suggest that AAV2/rh10 is a highly efficient serotype for gene delivery to mammalian photoreceptors, possibly providing an alternative to the frequently used AAV2/5 and AAV2/8 serotypes.

Interestingly, in this study, *RHO*-2/8 provided higher transgene expression levels at an earlier timepoint (1 week postsubretinal injection) than *RHO*-2/rh10 in the murine retina, indicating that the AAV2/8 serotype results in more rapid transgene expression in murine rod photoreceptor cells than the AAV2/rh10 serotype; however, expression levels from both serotypes are indistinguishable by 6 weeks post subretinal injection of vector (Figure 1b). Early high expression, such as that achieved from AAV2/8, may be of particular value when testing therapies in rapidly degenerating

disease models, such as the *RHO* Pro23His murine model of RP[30], among others. However, given the severe degenerating nature of the *Rho*–/– mouse model used and the fact that rescue was obtained using both serotypes, the results suggest that rhodopsin expression mediated by AAV2/rh10 was sufficient to preserve photoreceptors after early subretinal administration (p3-4) of vector. *RHO* mRNA levels in the treated *Rho*–/– retinas were ~75% of levels in NHR+/− *Rho*–/−[28,30] mice which express approximately the same level of rhodopsin mRNA as wild mice.[33]

In this study, rhodopsin delivery mediated by both AAV2/8 and AAV/rh10 serotypes provided histological (analyzed by light and electron microscopy) and functional benefits (analyzed by ERG and optomotry) to the *Rho*–/– mouse. Indeed, similar levels of rescue with these two serotypes were observed up to 11 months following treatment (Figures 2, 3, and 5–8). Although the rate of degeneration was reduced, ERG and histological analyses indicate that degeneration was not altogether arrested in treated mice. At this time it remains unclear what factor(s) are driving the retinal degeneration in the treated retinas. Because the treated area was up to approximately half of the total retinas, degeneration in the nontreated areas may have affected the treated regions. Notably, in a human gene therapy for LCA, while the therapy improved vision, the retinal degeneration was not stopped mirroring experiments in the canine model.[34]

In addition to the observed rescue of the cellular architecture with both serotypes, similar low numbers of infiltrating cells were observed in untreated retinas and retinas treated with either AAV2/8 or AAV/rh10. Presence of infiltrates in the untreated *Rho*–/– retina is possibly related to the ongoing degeneration of the tissue. As the number of infiltrates was low and did not increase in the treated retinas, these results suggest that the administered AAV load, both in terms of serotype and quantity, is well tolerated in the murine retina. Earlier, AAV2/rh10 has been shown to be well tolerated in other neuronal tissues in NHPs.[32] Furthermore, AAV2/rh10
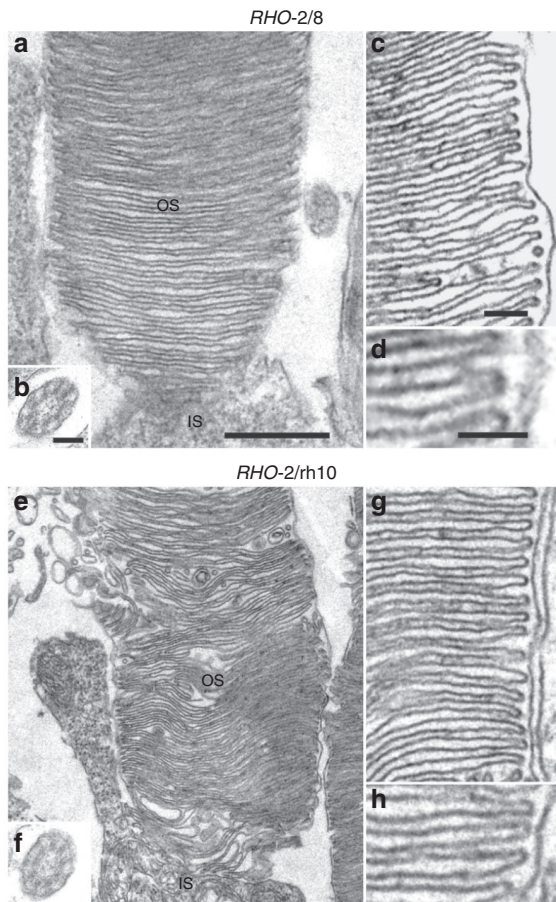
Gene delivery to photoreceptors using AAV2/rh10
A Palfi et al.

6

Figure 6 Ultrastructural analysis of rod photoreceptors in retinas transduced with *RHO*-2/8 and *RHO*-2/rh10 in *Rho*$^{-/-}$ mice. Eyes of *Rho*$^{-/-}$ mice were subretinally injected with 5×10^9 vg/eye of either (**a–d**) AAV2/8-BB24 (*RHO*-2/8) or (**e–h**) AAV2/rh10-BB24 (*RHO*-2/rh10) at p3-4. Both AAVs were mixed with 1×10^8 vg/eye of AAV2/5-EGFP tracer; untreated eyes served as controls (not shown). Eyes were fixed and retinas were whole mounted 6 months postinjection. Transduced areas of the retinas were identified by EGFP fluorescence; representative areas were excised, postfixed, and further processed for transmission electron microscopy. IS, rod inner segment; OS, rod outer segment. Connecting cilia (**b** and **f**) and correctly formed membrane disks (**c, d, g,** and **h**) were detected in the samples. Scale bar panel **a**: 1 μm; scale bar panels **b, c,** and **d**: 50 nm.

Figure 7 Rod-derived ERG analysis of *Rho*$^{-/-}$ mice treated with *RHO*-2/8 and *RHO*-2/rh10. Eyes of *Rho*$^{-/-}$ mice were subretinally injected with 5×10^9 vg/eye of either (**a**) AAV2/8-BB24 (*RHO*-2/8) or (**b**) AAV2/rh10-BB24 (*RHO*-2/rh10) at p3-4. Both AAVs were mixed with 1×10^8 vg/eye of AAV2/5-EGFP tracer; untreated eyes served as controls (not shown). Mice (*n* = 4–8) were dark-adapted overnight and rod-isolated ERG responses in 2, 5, and 11 months postinjection, *i.e.*, b-wave amplitudes recorded using a dim white flash (−25 dB of the maximal flash intensity where the maximal flash intensity was 3 candelas/m^2/s); corresponding ERG tracings are overlaid (**a** and **b**). Mean ERG amplitudes are presented in a bar chart (**c**). Error bars represent SD values. ***$P < 0.001$, **$P < 0.01$, *$P < 0.05$, compared with corresponding 2 months postinjections. *$P < 0.01$, compared with corresponding 5 months postinjection.

has been clinically tested in humans after intracerebral injection for mucopolysaccharidosis IIIA[35] and late infantile neuronal ceroid lipofuscinosis.[36] In an earlier study,[20] AAV2/rh10 was used to evaluate photoreceptor transduction after a p0 injection into the wild type mouse retina. Of note, in contrast to the efficient photoreceptor transduction and rescue of disease pathology obtained in this study using AAV2/rh10 in *Rho*$^{-/-}$ mice, photoreceptor transduction did not appear efficient, possibly because of the p0 delivery.[20]

Many gene therapies are now entering clinical trial with the first EU-approved AAV therapy, Glybera, having obtained market approval. This therapy utilizes AAV1 to administer the lipoprotein lipase gene to the muscle of patients with lipoprotein lipase deficiency. Other AAV gene therapies tested in recent clinical trials have also been well tolerated in patients when administered using a similar regimen of immunosuppression; immunological responses, where present, were of short duration with no lasting ill effects.[37,38] In the context of the retina, clinical trials to date for LCA and Choroideremia would suggest that AAV is well tolerated in
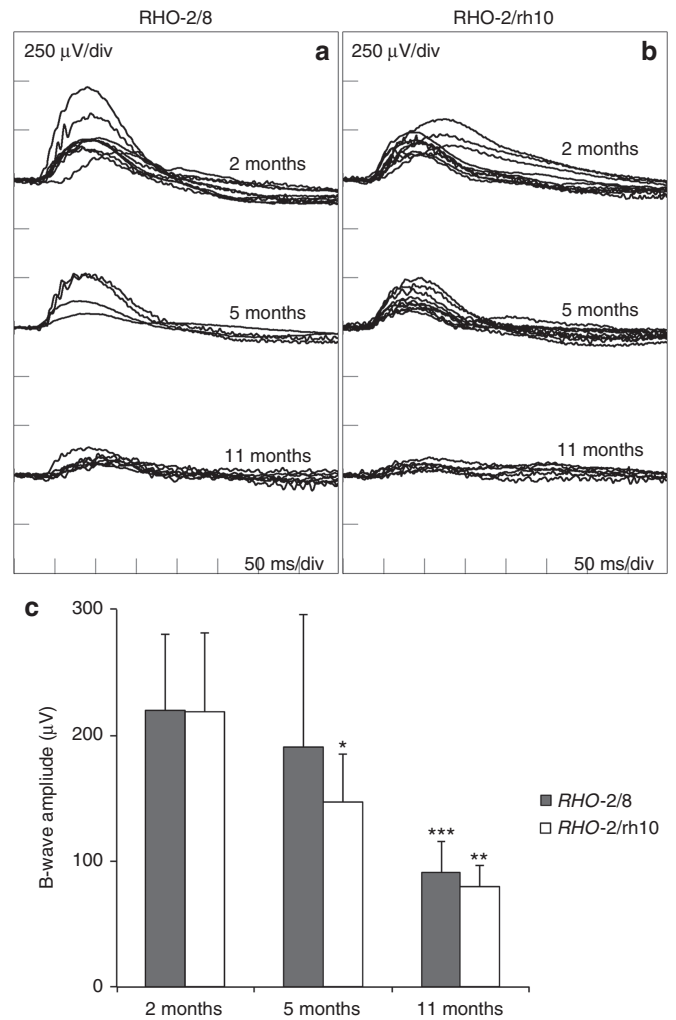
the human eye after subretinal administration.[1–3,6] Given the wide range of gene therapies for many different inherited ocular disorders currently in preclinical development,[39] there is a clear need for a repertoire of AAV vectors to deliver to this target tissue. Results from this study suggest that AAV2/rh10 should be considered as an efficient vector option for delivery to mammalian photoreceptors. Further studies in NHPs may be needed to identify the most optimal candidate serotype for gene transfer in humans.

Furthermore it is of note that recent studies employing gene delivery using AAV2/rh10 have demonstrated efficient dissemination and expression of the transgene throughout the spinal cord and certain regions of the brain.[23,32,40,41] Notably, retinal degenerations frequently present as part of the clinical symptoms of syndromic disorders. For example, symptoms of Usher
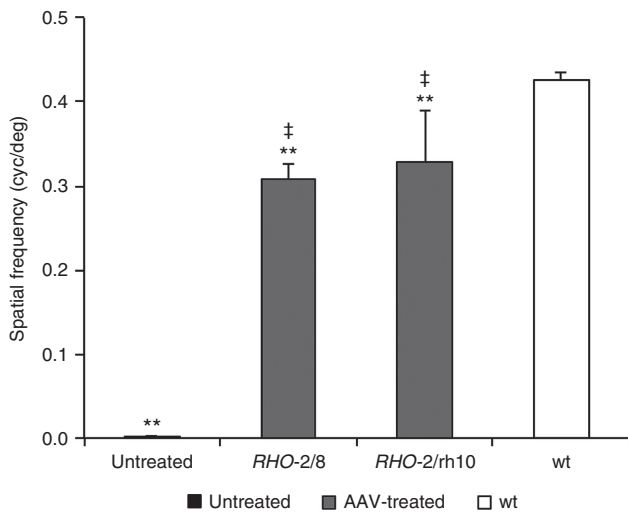
Gene delivery to photoreceptors using AAV2/rh10
A Palfi et al.

npg

7

Figure 8 Analysis of functional vision in *Rho*–/– mice treated with *RHO*-2/8 and *RHO*-2/rh10. Eyes of *Rho*–/– mice were subretinally injected with 5×10^9 vg/eye of either AAV2/8-BB24 (*RHO*-2/8) or AAV2/rh10-BB24 (*RHO*-2/rh10) at p3-4. Both AAVs were mixed with 1×10^8 vg/eye of AAV2/5-EGFP tracer; untreated eyes served as controls. The optokinetic tracking response (spatial frequency threshold) was measured using a virtual optokinetic system 6 months postinjection. Bar chart represents the mean spatial frequency threshold established for *RHO*-2/8 and *RHO*-2/rh10-treated (gray columns), age-matched untreated (black column), and wild-type mice (white column). Note that the untreated eyes had no tracking response and were assigned with a spatial frequency threshold of 0. Error bars represent SD values. $‡P < 0.01$ (compared with untreated eyes), $**P < 0.01$ (compared with wild-type eyes).

Syndrome include retinitis pigmentosa in conjunction with sensorineural deafness, whereas symptoms of Senior–Loken syndrome (a ciliopathy) include LCA, nephronophthisis, cerebellar ataxia, and skeletal abnormalities. For such disorders, dissemination of a gene therapeutic to multiple tissues and organs may be required. It is therefore of particular value to explore the various AAV serotype options that are available for such treatments. In this study, it has been established that AAV2/rh10 performs to a similar level as AAV2/8 in the context of gene delivery to mammalian photoreceptors. It has also been observed that AAV2/rh10 can efficiently transduce a variety of other neuronal targets, *e.g.*, in the brain and the spinal cord.[32,40,41] Indeed, in some of these cases, AAV2/rh10 has been shown to provide the highest levels of transgene expression, much higher than AAV2/8.[23,24] Therefore, AAV2/rh10 may represent an AAV serotype that has significant potential for gene therapies for multifaceted disorders, where photoreceptor degeneration represents one of a collection of disease phenotypes.

MATERIALS AND METHODS

AAV production

pAAV-BB24 and pAAV-*EGFP* were constructed as described.[29] Recombinant AAV-*EGFP* was generated using a helper virus-free system as described.[33] AAV2/8-BB24 (*RHO*-2/8) and AAV2/rh10-BB24 (*RHO*-2/rh10) were prepared in the Research Vector Core, University of Pennsylvania. AAV2/8 capsid (GenBank sequence AY242997) and AAV2/rh10 capsid Genomic titers (DNase-resistant viral genomes per milliliter; vg/ml) were determined by qPCR.[42]

Subretinal injections and RNA analysis

Subretinal injections were performed in compliance with the European Communities Regulations 2002 and 2005 (Cruelty to Animals Act) and the Association for Research in Vision and Ophthalmology statement for the use of animals in ophthalmic and vision research as described.[33] In brief, newborn (p3-4) mice were anesthetized as described.[43] A small puncture was made in the sclera. A 34-gage blunt-ended microneedle attached to a 10-µl syringe (Hamilton) was inserted through the puncture, 5×10^9 vg of AAV in 0.6 µl PBS was administered to the subretinal space, and retinal detachment was induced.[33] RNA was isolated from whole retinas 1 and 6 weeks postinjection and *RHO* expression analyzed by RT-qPCR as described.[33]

Histology

Eyes were fixed in 4% paraformaldehyde and processed for fluorescent microscopy analysis as described.[43] Rhodopsin immunohistochemistry was carried out using 4D2 antirhodopsin primary (1/100 dilution[30], provided by Dr. Robert Molday, Department of Biochemistry and Molecular Biology, University of British Columbia, Canada) and Cy3-conjugated anti-mouse secondary (1/400 dilution; Jackson Immuno Research, Newmarket, UK) antibodies. Rhodopsin label (Cy3), EGFP, and 4′,6-diamidino-2-phenylindole (DAPI) signals were detected by fluorescent microscopy as described[44]; corresponding images taken with different filter sets were overlaid. Hematoxylin and eosin staining was performed using Gill's hematoxylin and 1% alcoholic eosin Y. Histology measurements were carried out using Photoshop CS6 (Adobe Systems Software Ireland Ltd., Dublin, Ireland). Typically, images from two to three sections in the central part of the retina ~150 µm apart were analyzed in each eye.

Transmission electron microscopy analysis was performed as described.[29] In brief, eyes were fixed in 4% paraformaldehyde. Using the EGFP tracer, EGFP-positive areas from the central part of transduced retinas were excised and fixed in 2.5% glutaraldehyde in 0.1 M cacodylate buffer for 2 hours. Specimens were postfixed in 2% OsO_4 and embedded in Araldite. Ultrastructural analyses were performed with a Tecnai 12 Bio-TWIN transmission electron microscope (FEI, Eindhoven, the Netherlands) and imaged with an SIS MegaView III camera (Olympus Soft Imaging Solutions, Munster, Germany).

ERG

ERG measurements were performed as described.[45] In brief, animals were dark adapted overnight and procedures were carried out under dim red light. A mixture of ketamine and xylazine (16 and 1.6 µg/10 g body weight, respectively) were administered i.p. for anesthesia; pupils were dilated with 1% cyclopentalate and 2.5% phenylephrine. ERG responses were recorded simultaneously from both eyes by means of goldwire electrodes (Roland Consulting, Brandenburg-Wiesbaden, Germany). Standardized flashes of light were presented in a Ganzfeld bowl. Rod-isolated responses were recorded using a dim white flash (−25 dB of the maximal flash intensity, where the maximal flash intensity was 3 candelas/m²/s) presented in the dark-adapted state using a RetiScan RetiPort electrophysiology unit (Roland Consulting). Mixed rod/cone responses were then recorded to the maximal intensity flash (3 candelas/m²/s), presented in the dark-adapted state.

Optokinetic tracking response

Functional vision was tested using the optokinetic tracking response as described.[46] In brief, the spatial frequency thresholds (the point where the mouse no longer tracked the moving gratings) were determined by two independent researchers using a virtual optokinetic system (OptoMotry, CerebralMechanics, Lethbridge, AB, Canada).[31]

Statistical analysis

Mean and SD values of data sets were calculated. Statistical significance of differences between groups was determined using Mann–Whitney *U*-test, as normal distribution was not assumed (Data Desk 6.3.1, Data Description, New York); differences of $P < 0.05$ were considered statistically significant.

CONFLICT OF INTEREST

J.F. and P.K. are the directors of Genable Technologies. N.C., A.P., and S.M.-W. are the consultants for Genable Technologies. M.O. is a former consultant for Genable

REFERENCES

1. Bainbridge, JW, Smith, AJ, Barker, SS, Robbie, S, Henderson, R, Balaggan, K *et al.* (2008). Effect of gene therapy on visual function in Leber's congenital amaurosis. *N Engl J Med* **358**: 2231–2239.

2. Maguire, AM, Simonelli, F, Pierce, EA, Pugh, EN Jr, Mingozzi, F, Bennicelli, J *et al.* (2008). Safety and efficacy of gene transfer for Leber's congenital amaurosis. *N Engl J Med* **358**: 2240–2248.

3. Hauswirth, W, Aleman, TS, Kaushal, S, Cideciyan, AV, Schwartz, SB, Wang, L *et al.* (2008). Phase I trial of Leber congenital amaurosis due to RPE65 mutations by ocular subretinal injection of adeno-associated virus gene vector: short-term results. *Hum Gene Ther* **19**: 979–990.

4. Bennett, J (2003). Immune response following intraocular delivery of recombinant viral vectors. *Gene Ther* **10**: 977–982.

5. Willett, K and Bennett, J (2013). Immunology of AAV-mediated gene transfer in the eye. *Front Immunol* **4**: 261.

6. MacLaren, RE, Groppe, M, Barnard, AR, Cottriall, CL, Tolmachova, T, Seymour, L *et al.* (2014). Retinal gene therapy in patients with choroideremia: initial findings from a phase ½ clinical trial. *Lancet* **383**: 1129–1137.

7. Auricchio, A, Kobinger, G, Anand, V, Hildinger, M, O'Connor, E, Maguire, AM *et al.* (2001). Exchange of surface proteins impacts on viral vector cellular specificity and transduction characteristics: the retina as a model. *Hum Mol Genet* **10**: 3075–3081.

8. Rabinowitz, JE, Rolling, F, Li, C, Conrath, H, Xiao, W, Xiao, X *et al.* (2002). Cross-packaging of a single adeno-associated virus (AAV) type 2 vector genome into multiple AAV serotypes enables transduction with broad specificity. *J Virol* **76**: 791–801.

9. Gao, G, Wilson, JM and Alvira, A (2002). Adeno-associated virus (AAV) serotype rh10. European Patent EP2341068B1.

10. Gao, GP, Alvira, MR, Wang, L, Calcedo, R, Johnston, J and Wilson, JM (2002). Novel adeno-associated viruses from rhesus monkeys as vectors for human gene therapy. *Proc Natl Acad Sci USA* **99**: 11854–11859.

11. Maheshri, N, Koerber, JT, Kaspar, BK and Schaffer, DV (2006). Directed evolution of adeno-associated virus yields enhanced gene delivery vectors. *Nat Biotechnol* **24**: 198–204.

12. Koerber, JT, Jang, JH and Schaffer, DV (2008). DNA shuffling of adeno-associated virus yields functionally diverse viral progeny. *Mol Ther* **16**: 1703–1709.

13. Lebherz, C, Maguire, A, Tang, W, Bennett, J and Wilson, JM (2008). Novel AAV serotypes for improved ocular gene transfer. *J Gene Med* **10**: 375–382.

14. Koerber, JT, Klimczak, R, Jang, JH, Dalkara, D, Flannery, JG and Schaffer, DV (2009). Molecular evolution of adeno-associated virus for enhanced glial gene delivery. *Mol Ther* **17**: 2088–2095.

15. Dalkara, D, Byrne, LC, Klimczak, RR, Visel, M, Yin, L, Merigan, WH *et al.* (2013). In vivo-directed evolution of a new adeno-associated virus for therapeutic outer retinal gene delivery from the vitreous. *Sci Transl Med* **5**: 189ra76.

16. Cronin, T, Vandenberghe, LH, Hantz, P, Juttner, J, Reimann, A, Kacsó, AE *et al.* (2014). Efficient transduction and optogenetic stimulation of retinal bipolar cells by a synthetic adeno-associated virus capsid and promoter. *EMBO Mol Med* **6**: 1175–1190.

17. Zinn, E and Vandenberghe, LH (2014). Adeno-associated virus: fit to serve. *Curr Opin Virol* **8**: 90–97.

18. Reich, SJ, Auricchio, A, Hildinger, M, Glover, E, Maguire, AM, Wilson, JM *et al.* (2003). Efficient trans-splicing in the retina expands the utility of adeno-associated virus as a vector for gene therapy. *Hum Gene Ther* **14**: 37–44.

19. Surace, EM, Auricchio, A, Reich, SJ, Rex, T, Glover, E, Pineles, S *et al.* (2003). Delivery of adeno-associated virus vectors to the fetal retina: impact of viral capsid proteins on retinal neuronal progenitor transduction. *J Virol* **77**: 7957–7963.

20. Watanabe, S, Sanuki, R, Ueno, S, Koyasu, T, Hasegawa, T and Furukawa, T (2013). Tropisms of AAV for subretinal delivery to the neonatal mouse retina and its application for *in vivo* rescue of developmental photoreceptor disorders. *PLoS One* **8**: e54146.

21. Bruewer, AR, Mowat, FM, Bartoe, JT, Boye, SL, Hauswirth, WW and Petersen-Jones, SM (2013). Evaluation of lateral spread of transgene expression following subretinal AAV-mediated gene delivery in dogs. *PLoS One* **8**: e60218.

22. Allocca, M, Mussolino, C, Garcia-Hoyos, M, Sanges, D, Iodice, C, Petrillo, M *et al.* (2007). Novel adeno-associated virus serotypes efficiently transduce murine photoreceptors. *J Virol* **81**: 11372–11380.

23. Cearley, CN and Wolfe, JH (2006). Transduction characteristics of adeno-associated virus vectors expressing cap serotypes 7, 8, 9 and Rh10 in the mouse brain. *Mol Ther* **13**: 528–537.

24. Hu, C, Busuttil, RW and Lipshutz, GS (2010). RH10 provides superior transgene expression in mice when compared with natural AAV serotypes for neonatal gene therapy. *J Gene Med* **12**: 766–778.

25. Sondhi, D, Johnson, L, Purpura, K, Monette, S, Souweidane, MM, Kaplitt, MG *et al.* (2012). Long-term expression and safety of administration of AAVrh.10hCLN2 to the brain of rats and nonhuman primates for the treatment of late infantile neuronal ceroid lipofuscinosis. *Hum Gene Ther Methods* **23**: 324–335.

26. Giove, TJ, Sena-Esteves, M and Eldred, WD (2010). Transduction of the inner mouse retina using AAVrh8 and AAVrh10 via intravitreal injection. *Exp Eye Res* **91**: 652–659.

27. Mao, Y, Kiss, S, Boyer, JL, Hackett, NR, Qiu, J, Carbone, A *et al.* (2011). Persistent suppression of ocular neovascularization with intravitreal administration of AAVrh.10 coding for bevacizumab. *Hum Gene Ther* **22**: 1525–1535.

28. Humphries, MM, Rancourt, D, Farrar, GJ, Kenna, P, Hazel, M, Bush, RA *et al.* (1997). Retinopathy induced in mice by targeted disruption of the rhodopsin gene. *Nat Genet* **15**: 216–219.

29. Palfi, A, Millington-Ward, S, Chadderton, N, O'Reilly, M, Goldmann, T, Humphries, MM *et al.* (2010). Adeno-associated virus-mediated rhodopsin replacement provides therapeutic benefit in mice with a targeted disruption of the rhodopsin gene. *Hum Gene Ther* **21**: 311–323.

30. Olsson, JE, Gordon, JW, Pawlyk, BS, Roof, D, Hayes, A, Molday, RS *et al.* (1992). Transgenic mice with a rhodopsin mutation (Pro23His): a mouse model of autosomal dominant retinitis pigmentosa. *Neuron* **9**: 815–830.

31. Douglas, RM, Alam, NM, Silver, BD, McGill, TJ, Tschetter, WW and Prusky, GT (2005). Independent visual threshold measurements in the two eyes of freely moving rats and mice using a virtual-reality optokinetic system. *Vis Neurosci* **22**: 677–684.

32. Yang, B, Li, S, Wang, H, Guo, Y, Gessler, DJ, Cao, C *et al.* (2014). Global CNS transduction of adult mice by intravenously delivered rAAVrh.8 and rAAVrh.10 and nonhuman primates by rAAVrh.10. *Mol Ther* **22**: 1299–1309.

33. O'Reilly, M, Millington-Ward, S, Palfi, A, Chadderton, N, Cronin, T, McNally, N *et al.* (2008). A transgenic mouse model for gene therapy of rhodopsin-linked retinitis pigmentosa. *Vision Res* **48**: 386–391.

34. Cideciyan, AV, Jacobson, SG, Beltran, WA, Sumaroka, A, Swider, M, Iwabe, S *et al.* (2013). Human retinal gene therapy for Leber congenital amaurosis shows advancing retinal degeneration despite enduring visual improvement. *Proc Natl Acad Sci USA* **110**: E517–E525.

35. Tardieu, M, Zérah, M, Husson, B, de Bournonville, S, Deiva, K, Adamsbaum, C *et al.* (2014). Intracerebral administration of adeno-associated viral vector serotype rh.10 carrying human SGSH and SUMF1 cDNAs in children with mucopolysaccharidosis type IIIA disease: results of a phase I/II trial. *Hum Gene Ther* **25**: 506–516.

36. Crystal, RG and Bethesda, MD. Recombinant DNA Advisory Committee, National Institutes of Health, 2009.

37. Ferreira, V, Twisk, J, Kwikkers, K, Aronica, E, Brisson, D, Methot, J *et al.* (2014). Immune responses to intramuscular administration of alipogene tiparvovec (AAV1-LPL(S447X)) in a phase II clinical trial of lipoprotein lipase deficiency gene therapy. *Hum Gene Ther* **25**: 180–188.

38. Testa, F, Maguire, AM, Rossi, S, Pierce, EA, Melillo, P, Marshall, K *et al.* (2013). Three-year follow-up after unilateral subretinal delivery of adeno-associated virus in patients with Leber congenital Amaurosis type 2. *Ophthalmology* **120**: 1283–1291.

39. Farrar, GJ, Millington-Ward, S, Chadderton, N, Mansergh, FC and Palfi, A (2014). Gene therapies for inherited retinal disorders. *Vis Neurosci* **31**: 289–307.

40. Swain, GP, Prociuk, M, Bagel, JH, O'Donnell, P, Berger, K, Drobatz, K *et al.* (2014). Adeno-associated virus serotypes 9 and rh10 mediate strong neuronal transduction of the dog brain. *Gene Ther* **21**: 28–36.

41. Holehonnur, R, Luong, JA, Chaturvedi, D, Ho, A, Lella, SK, Hosek, MP *et al.* (2014). Adeno-associated viral serotypes produce differing titers and differentially transduce neurons within the rat basal and lateral amygdala. *BMC Neurosci* **15**: 28.

42. Rohr, UP, Wulf, MA, Stahn, S, Steidl, U, Haas, R and Kronenwett, R (2002). Fast and reliable titration of recombinant adeno-associated virus type-2 using quantitative real-time PCR. *J Virol Methods* **106**: 81–88.

43. Matsuda, T and Cepko, CL (2004). Electroporation and RNA interference in the rodent retina *in vivo* and *in vitro*. *Proc Natl Acad Sci USA* **101**: 16–22.

44. Chadderton, N, Millington-Ward, S, Palfi, A, O'Reilly, M, Tuohy, G, Humphries, MM *et al.* (2009). Improved retinal function in a mouse model of dominant retinitis pigmentosa following AAV-delivered gene therapy. *Mol Ther* **17**: 593–599.

45. Kiang, AS, Palfi, A, Ader, M, Kenna, PF, Millington-Ward, S, Clark, G *et al.* (2005). Toward a gene therapy for dominant disease: validation of an RNA interference-based mutation-independent approach. *Mol Ther* **12**: 555–561.

46. Chadderton, N, Palfi, A, Millington-Ward, S, Gobbo, O, Overlack, N, Carrigan, M *et al.* (2013). Intravitreal delivery of AAV-NDI1 provides functional benefit in a murine model of Leber hereditary optic neuropathy. *Eur J Hum Genet* **21**: 62–68.

Supplementary Information accompanies this paper on the *Molecular Therapy—Methods & Clinical Development* website (http://www.nature.com/mtm)